

# Characterization of Wire Rope Defects from Magnetic Flux Leakage Signals

**C.Jomdecha**

Non-Destructive Testing Technology Center

**A.Prateepasen and W.Methong**

Non-Destructive Testing Technology Center

Production Engineering Department, Faculty of Engineering,

King Mongkut's University of Technology Thonburi

91 Prachautid, Bangmod, Toongkru, Bangkok, Thailand 10140.

Tel: 66-0-2470-9679; Fax: 66-0-2470-9681; Email: iasaasen@kmutt.ac.th

## Abstract

When using magnetic flux leakage to inspect wire rope, two types of signals are produced for analysis, namely: Localized Fault (LF) and Loss of Magnetic Cross-section Area (LMA). However, these signals contain a lot of other noises which makes the defects difficult to perfectly analyze. Therefore, this paper is written to characterize and analyze signals of the wire rope defects obtained from the magnetic flux leakage equipment. The implementation of a wavelet transform is the main goal to characterize the wire rope inspection signal. The advantages are able to represent the defect locations in time-frequency domain based, de-noise and decompose the different frequency constituents. Time and frequency localizations of the defects then can be explored by using the continuous wavelet transform to enhance a visualization of the inspection signal. The discrete wavelet transform is implemented for de-noising as a result of the frequency constituent decompositions.

**Keyword:** Wire rope defect, Magnetic flux leakage, Characterization, De-noising, Wavelet transform

## 1. Introduction

Wire ropes are used for various applications such as cable-stayed bridges, lifts, cranes and cable cars. Deterioration of the wire rope causes the declination of the structure strength. Types of imperfection or defect, for instance wire breakage, corrosion, abrasion or wear which cause the wire rope to degrade and eventually become destroyed are reviewed in this study [1]. Numerous Non-Destructive Testing (NDT) methods have been employed to inspect the wire rope including visual inspection, magnetic flux leakage, radiographic testing and imaging method, but the two most conventional approaches are the visual inspection and the magnetic flux leakage [2].

The Magnetic Flux Leakage (MFL) inspection is appropriate for the wire rope inspection due to its high accuracy and resolution [2-4]. Flux leakage from the defects

in the wire ropes can be detected by using a coil or hall sensor. The signals obtained from sensors can be divided in two types; localized fault (LF) and loss of metallic cross-section area (LMA). The LF trace is operated to locate the defects whereas the LMA trace is performed to measure an accurate loss of the diameter of the wire rope. The signal of the flux leakage received from the defect oscillates with different amplitude and duration time. It consists of various frequency components. In addition the associated noise caused by vibration of the wire rope and the signal variation due to the gap between the wire rope and the MFL instrument, MFL instrument, suitable signal processing techniques for the MFL inspection signals are needed to analyze signal characterization. Several studies refer to advanced signal processing for MFL signal to characterize defects by using digital signal processing and signal correlation technique.

A part of the content has appeared and been discussed at the 25<sup>th</sup> Electrical Engineering Conference (EECON-25), on 21-22 Nov.2002 held at Prince of Songkla University, Hat Yai, Songkla, Thailand.

Recently, the wavelet transform is revealed to be a useful tool for analyzing the signal in a wide variety of applications. Time localization and scale based with resolution are presented in this transform. They are applied to analyze many applications such as heart pulse signals, bursts in electrical system or acoustical signals. The intention is to process the tested signal to the different frequencies with different scaled resolutions. In the MFL applications the wavelet transform either continuous or discrete is also implemented to analyze the flux leakage signals of a pipeline or wire rope [5-8]. Dissimilarities of the signal can be explored for detection and categorization the defects characters.

In this paper, the design and construction of the MFL equipment is shown and both continuous and discrete wavelet transform are implemented. Consequently, the flux leakage results are exhibited in the different presentation that is easy to distinguish and increase time-frequency locations detail of the inspection signal. Therefore the defects of the wire rope can be categorized and investigated in different frequencies and localizations.

## 2. Magnetic flux leakage inspection

The MFL is implemented by applying magnetic field intensity to a ferromagnetic material specimen. Poles of the magnet are produced to exert forces on a specimen. This attraction force is caused by the magnetic field. Amount of magnetic flux show the strength and direction of magnetic field intensity. A large number of the flux lines correspond to the strong magnetic field. It can be produced with a well-known equation

$$B = \mu H \tag{1}$$

Whereas B is the magnetic field density, H is the magnetic field intensity and  $\mu$  is the magnetic permeability of material. The operation principle of the MFL equipment is applying a direct current or permanent magnets to supply the high constant magnetic field throughout the length of the wire rope. The magnetic flux that leaks from a discontinuity in the rope, such as a broken wire, can be detected with a differential sensor, such as a Hall Effect sensor, coil sensor or by any appropriate device. The signal from the sensor is electrically processed and recorded. Localized faults can be

located and loss of metallic cross-section area can be evaluated in the cross-section areas of the wire rope.

The MFL equipment has been designed and constructed in the previous work [9-11]. The electromagnet is used to apply the magnetic field to the wire rope in order to interact with the artificial flaws to produce flux leakage. The diagram of the system is shown in Figure 1. The three restrictions that need to be taken into consideration are firstly, the magnetic field density must be strong enough to measure the amount of the flux leakage seepage from the flaws. Secondly, the inspection area must be covered both inside and on the surface of the wire rope. Lastly the measurement results can be compared at different locations while the equipment runs along the length of the wire rope.

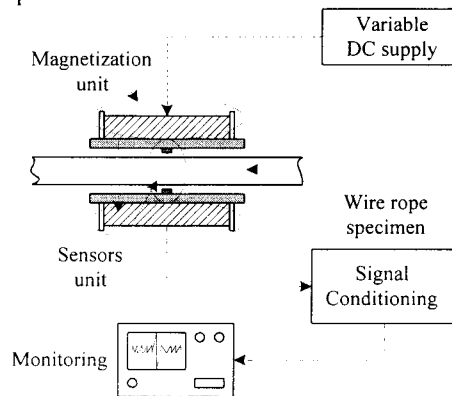


Figure 1 The magnetic flux leakage equipment

For detecting the magnetic flux leakage, induction coils and hall sensor [12] are appropriated to use in MFL system. These sensors work on different physical principles. In equations (2) and (3), the relations between the electrical quantity output and the magnetic flux leakage to be measured are shown.

For the induction coils:

$$V = n \frac{d\Phi}{dt} \tag{2}$$

Where  $V$  = Output voltages  
 $n$  = Turns of coil  
 $d\Phi$  = Derivative of the magnetic flux  
 $dt$  = Derivative of times

For the Hall Sensors:

$$V = \frac{I \times B}{nqt} \quad (3)$$

Where  $V$  = Output voltages of the hall sensor

- $I$  = Hall sensor current
- $B$  = Magnetic field density of MFL
- $n$  = Density of charge carriers
- $q$  = Electric charge
- $t$  = Hall sensor thickness

The induction coils are selected to use in the MFL equipment. They were made of 40 AWG coil in printed-circuit-shape. The advantages of the induction coils are that they are not sensitive to the strong background fields and are suitable for high temperature environment. Additionally, in case of the sensors being connected in series, noises from the variation of the peak to valley of the wire rope surface can be reduced. As the result of the flux leakage is a vector field that consists of three unique components [13]. They refer to the axial, radial, and tangential direction. The flux density at the metal loss region  $\vec{B}_o$  is the result of an equation (4) as follows:

$$\vec{B}_o = \vec{B}_{ot} + \vec{B}_{or} + \vec{B}_{os} \quad (4)$$

Where  $\vec{B}_{ot}$ ,  $\vec{B}_{or}$  and  $\vec{B}_{os}$  are resolved vectors in the axial, radial and tangential direction respectively. Hence the sensor shape and its orientation are the important factors. In the research, coil sensor in printed-circuit-shape was chosen because it can be used to measure the total flux leakage in all directions. The sensor shape was designed in a small size in order for ease of mounting to the equipment. The sensor orientation was arranged appropriately at the center of the equipment to detect the flux leakage. The inspection signal was the product of electrical signal as a result of the total flux leakage in the axial, radial and tangential directions. The sensor shape, its orientation and

the directions of  $\vec{B}_{ot}$ ,  $\vec{B}_{or}$ ,  $\vec{B}_{os}$  are as shown in Figure 2.

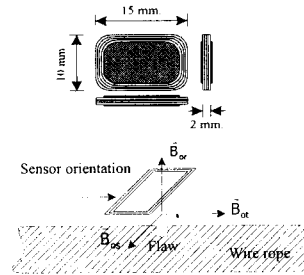


Figure 2 sensor shape and its orientation

### 3. LF/ LMA and corresponding signal

The principle deterioration modes of the wire rope inspection using MFL [14] can be categorized as follows:

#### Localized Faults (LF)

Discontinuities of the wire rope, such as broken or damaged wires, corrosion pits on the wire rope, grooves worn into the wire rope or any other physical conditions that degrade the integrity of the wire rope in a localized manner.

#### Loss of Metallic cross-section Area (LMA)

A relative measure of the amount of material (mass) missing from a location along the wire rope and is measured by comparing a point with a reference point on the wire rope that represents.



Figure 3 LF and LMA signals of wire rope

For localized fault inspection, defect locations of the wire rope are represented. The character of the defect signal is an impulse of electrical signal which is higher in amplitude than ordinary signal. Therefore the levels of deterioration of the wire rope can be presented by comparing the height of the amplitudes between the impulse signals. The significant consideration of the LF signal is the measurement ability such as resolution,

repeatability, and sensitivity of the MFL equipment. Usually, the LF signal is the main function of the MFL equipment. Although, it is used to define the measurement ability of the equipment, the length or depth of defect cannot be offered. Thus the loss of metallic cross-section area (LMA) signal is assisted to define a relative of the defect length and depth. The relative of the LMA signal is implemented to define the quantitative fault of the wire rope by using the quantitative resolution of the equipment. The quantitative resolution is the required minimum length of the uniform flaw for which the sensor provides an accurate quantitative measurement within a predefined small error limit. Because the quantitative resolution is finite in all sensors, minimum flaw lengths are always required to accurate quantitative fault identification. It is important for specifying and comparing the performance of MFL equipment. Figure 4 represents the comparing of the quantitative resolution of two equipment. Figure 4A shows the equipment with the quantitative resolution of 5 cm. that can determine the exact 10% of the LMA by this defect. On the other hand is as shown in Figure 4B, the result of the % LMA is about  $\frac{5}{30} \times 10 \approx 1.7\%$  on the same defect when using the equipment of the quantitative resolution of 30 cm.

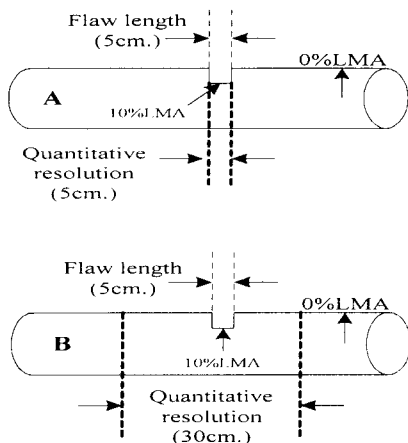


Figure 4. Comparing the quantitative resolution of the equipment

The test specimen 8×19(outer strand×wire) rope is used for testing. The eight outer strands

are manufactured in right ray, with the inner strands being left lay. Figure 5 shows artificial defects of the testing rope made for testing by the magnetic flux leakage equipment.

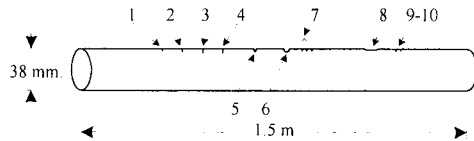


Figure 5 The wire rope test specimen

1, 2, 3 and 4 represent the variation of the depth of defects with the constant width of 1 mm. They are 2.5, 3.5, 4.5 and 5.5 mm respectively. 5 and 6 are wide defects of 3 and 5 mm. with 2.5 mm. depth, 7 is a group of 5 defects. 8 is the defect caused by wear. 9-10 are 2 defects for testing the resolution of the instrument.

The inspection results of the equipment present a performance of the dual function equipment (LF/LMA signals). They were verified the capability to detect the defects of a wire rope specimen. The performance can be displayed which are good repeatability, fine resolution at 2-cm. width and high sensitivity at 2-mm. depth of defect. The result of LF/LMA inspection is shown in Figure 6

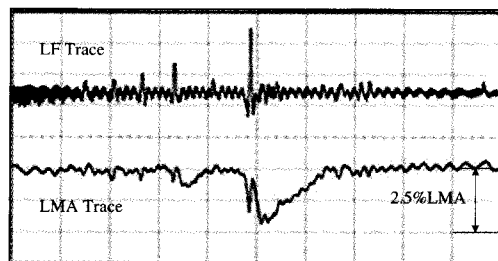


Figure 6 The dual function of the magnetic flux leakage equipment

In Figure 6, the LF and LMA signals can be displayed in the monitor simultaneously. The LF signal demonstrates the locations and the deterioration levels of the wire rope. The LMA signal establishes the relative of loss metallic cross-section area by integration the LF signal to approximate the loss metal region. The LMA result reveals the quantitative resolution of the equipment is 2 cm. The relative value of actual

10%LMA at the defect length of 5 mm. can be estimated a metal loss area of  $\frac{5}{20} \times 10 = 2.5\%$  by this equipment.

The difficulty to investigate and identify the LF/LMA is the signals obtained are complex on account of accompanying noises. They were affected from the variation of the peak-to-valley of the wire rope surface, electromagnetic disturbance and analog electronic circuits. From the LF signal in Figure 5, the averaging signal utility of the Digital Storage Oscilloscope (DSO) was used to facilitate for ease of considering the inspection signal. The consequence of averaging signal is demonstrated in Figure 7.

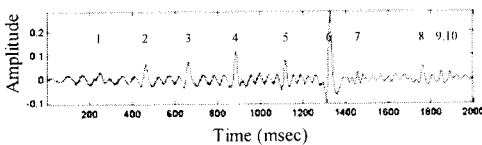


Figure 7 LF signal with averaging utility

Although the result of average signal can be assisted to investigate the defect signals, the noises are still contained in the inspection signal. The spectra of the inspection signal is as shown in Figure 8, it demonstrated the frequency component of the inspection signal. Because the high-frequency constituents of noises are contained in the signal at 150 and 300 Hz., the defects are difficult to analyze. Therefore several signal processing techniques were used to characterize and de-noise the MFL inspection signals. The wavelet transform implementation was then used to analyze the LF inspection signal in this paper. The continuous and discrete wavelet transform techniques were utilized to categorize and de-noise signals in time-scale presentations, by using a Symlet family wavelet basis function for which the defects were effortlessly investigated.

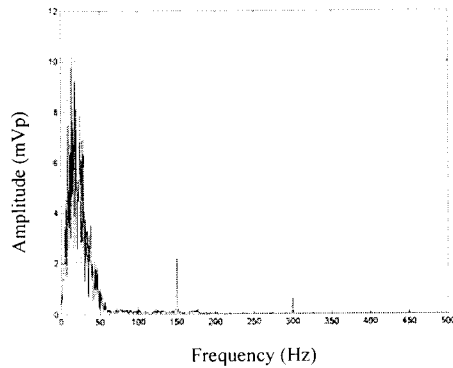


Figure 8 Frequency spectra of the inspection signal

#### 4. Approach with wavelet transform

The wavelet transform [15-17] is probably solution to overcome the shortcoming of the Fourier transform. In wavelet analysis the use of a fully modulated window can solve the signal-cutting problem. The window is shifted along the signal and for every position of the spectra is calculated. This process is repeated many times with a slightly shorter or longer window for every new cycle. The result is exhibited in a collection of the time-frequency presentations of the signal with different resolutions. In the wavelet transform, the time-scale presentations is replaced of the time-frequency presentations because the term frequency is reserved for the Fourier transform which the scale is in a way the opposite of frequency.

The most important properties of wavelets are admissibility and regularity conditions. These are the properties which are given their wavelet name. It can be shown as the square integration function  $\psi(t)$  satisfying the admissibility condition is

$$\int \frac{|\Psi(\omega)|^2}{|\omega|} d\omega < +\infty \quad (5)$$

It can be used to first analyze and then reconstruct a signal without loss of information. In equation (5)  $\Psi(\omega)$  stands for the Fourier transforms of  $\psi(t)$ . The admissibility condition is implied that the Fourier transforms  $\psi(t)$  vanished at the zero frequency follow as

$$\begin{aligned} |\Psi(\omega)|^2|_{\omega=0} &= 0 \\ (6) \\ \int \psi(t)dt &= 0 \end{aligned} \quad (7)$$

Equations (6) and (7) mean that the wavelet must have a band-pass like spectrum. This is a very important observation, which is used later to build an efficient wavelet transform. A zero at the zero frequency also means that the average value of the wavelet in the time domain must be zero. Therefore it must be oscillatory, in other words  $\psi(t)$  must be a wave.

**The continuous wavelet transform**

The continuous wavelet transform (CWT) was developed as an alternative to the short time Fourier transform (STFT) to overcome the resolution problem. The CWT is done in a similar way to the STFT analysis, in the sense that the signal is multiplied with a function, similar to the window function in the STFT and the transform is computed separately for different segments of the time-domain signal. However, the difference between the STFT and the CWT is the width of the CWT windowed changed as the transform is computed for every single spectral component, which is properly used as the most significant characteristic of the wavelet transform. The CWT is described in the introduction is written as

$$\gamma(s, \tau) = \int f(t)\psi^*_{s,\tau}(t)dt \quad (8)$$

Where \* is a complex conjugation. This equation shows a function  $f(t)$  is decomposed into a set of basis function  $\psi_{s,\tau}(t)$ , its called the wavelet. The variables  $s$  and  $\tau$  represent the new dimensions, namely scale and translation, which are introduced after the wavelet transform. For completeness equation (9) is given the inverse wavelet transform.

$$f(t) = \iint \gamma(s, \tau)\psi_{s,\tau}(t)d\tau ds. \quad (9)$$

The wavelets generated from a single basic wavelet  $\psi(t)$  are called mother wavelet, by scaling and translation as follows:

$$\psi_{s,\tau}(t) = \frac{1}{\sqrt{s}} \psi\left(\frac{t-\tau}{s}\right) \quad (10)$$

In an equation (10)  $s$  is the scale, factor  $\tau$  is the translation factor and the factor  $\frac{1}{\sqrt{s}}$  is the

energy normalization across the different scale. It is important to note that in equations (8), (9) and (10) the wavelet basis functions are not specified. This is a difference between the wavelet transform and the Fourier transform, or other transforms. The wavelet transform of a one-dimensional function is two-dimensional; the wavelet transform of a two-dimensional function is four-dimensional. These are the properties of the wavelet transform which are smoothness and concentration in both time and frequency domains.

**The discrete wavelet transform**

The discrete wavelet transform (DWT) is used to transform the continuous signal, the result is a series of wavelet coefficients, and it is referred to as the wavelet decomposition. The DWT is utilized to remove a redundancy of the CWT for which the CWT is calculated by continuously shifting a scalable function over a signal and calculating the correlation between the scale and the signal. It is obvious that the scaled function is near the basis function and obtained the highly redundant wavelet coefficients. In the DWT, the scaling function  $\phi(t)$  can be expressed up to a scale  $j$  in the multi-resolution or two scale relations follow an equation (11).

$$\phi(2^j t) = \sum_k h_{j+1}(k)\phi(2^{j+1}t - k) \quad (11)$$

The scaling function at the scale  $j$  can be expressed in terms of translated the scaling function at the next smaller or more detail. The first scaling function replaces a set of wavelets and also articulates the wavelet in this set in terms of translated scaling function at the next scale. More specifically, the wavelet can be written at level  $j$  in an equation (12).

$$\psi(2^j t) = \sum_k g_{j+1}(k)\phi(2^{j+1}t - k) \quad (12)$$

If a signal  $f(t)$  can be expressed in terms of dilated and translated wavelet up to a scale  $j-1$ , the result of  $f(t)$  can also be expressed in terms

of dilated and translated scaling functions at a scale  $j$  as an equation (13).

$$f(t) = \sum_k \lambda_j(k) \varphi(2^j t - k) \quad (13)$$

In equation (13) the scale can be stepped up to  $j-1$ . The wavelets are added in order to keep the same level of signal detail. Therefore, the signal  $f(t)$  can be expressed as

$$f(t) = \sum_k \lambda_{j-1}(k) \varphi(2^{j-1} t - k) + \sum_k \gamma_{j-1}(k) \psi(2^{j-1} t - k) \quad (14)$$

If the scaling function  $\varphi_{j,k}(t)$  and the wavelet  $\psi_{j,k}(t)$  are orthonormal functions, the wavelet coefficients  $\lambda_{j-1}(k)$  and  $\gamma_{j-1}(k)$  are found by taking the inner products.

$$\lambda_{j-1}(k) = [f(t), \varphi_{j,k}(t)] \text{ and } \gamma_{j-1}(k) = [f(t), \psi_{j,k}(t)] \quad (15)$$

From equation (15), the  $\varphi_{j,k}(t)$  and  $\psi_{j,k}(t)$  can be replaced in the inner products by suitably scaled and translated versions of the equations (11) and (12). The product can also be written as an integration result in equation (16).

$$\lambda_{j-1}(k) = \sum_m h(m - 2k) \lambda_j(m) \text{ and } \gamma_{j-1}(k) = \sum_m g(m - 2k) \gamma_j(m) \quad (16)$$

The equation (16) circumstantiates that the wavelet and the scaling function coefficients can calculate a weighted sum of the coefficients from the previous scale. The filters  $h(k)$  and  $g(k)$  of the different cutoff frequency are used to analyze the signal  $f(t)$  in different scales. The signal is passed through the high-pass filter  $g(k)$  to analyze the high frequency, and it is passed through the low-pass filter  $h(k)$  to analyze the low frequency. In Figure 9, the equation (16) can be implemented as one stage of an iterated filter bank in low-pass and high-pass filters with down-sampling of the signal.

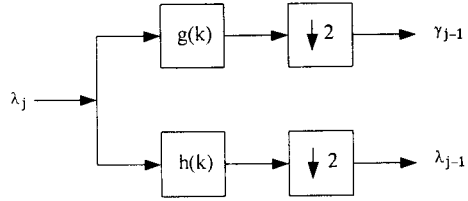


Figure 9 Implementation of the DWT as one stage of an iterated filter bank

### 5. Results and discussion

The MFL signal was implemented to analyze by using the symlet basis function [18] in the wavelet transform. It is appropriated for the signal that provides impulse localization in different scales. The symlets family is orthogonal and compactly supported wavelets which are nearly symmetrical. They were proposed by Daubechies as modifications to the db family. Because the MFL signals are impulse in different amplitudes and duration times which is poor regularity, the wavelet basis function that is compactly supported near symmetrically and has also vanishing moment can be implemented in this case. Therefore, the symlet basis function was selected to enhance the visualization of the defects character. Figure 10 demonstrates the symlets family.

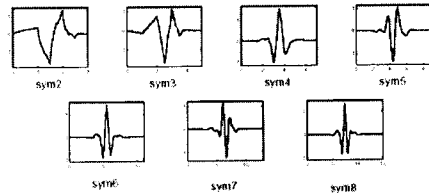


Figure 10 The symlet family

### Characterization by CWT

The proposal to use the continuous wavelet transform is distinguished by the MFL wire rope inspection signal in time-scale presentations and analyzed the characterization of the defects impulse signals. The result of characterization is shown in Figure 11. The result has shown the different wavelet coefficient amplitudes of the defects impulse signals.

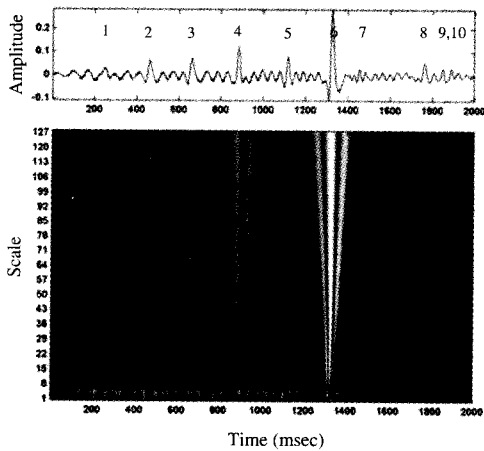


Figure 11 The wire rope defects characterization using CWT

The difference is easily visualized the summarization at the high scale (low frequency) and the details of the defects can be determined at the low scale (high frequency). The 10 defects with different localization were analyzed by continuous wavelet transform with symlet 6 in 128 different scales. The time-scale presentations are used to demonstrate the ease of visualization of the defects. Note that at the low scale, the high wavelet coefficient has appeared. It has been produced as the noises along the time localization from beginning of the inspection to about 1400 msec. The advantage of CWT is able to show details of the signal in two-dimension (time and scale). Therefore the impulse of defects can be characterized in different visualization in scale and time localization.

In CWT analysis, the wavelet coefficients were calculated in every scale as full amount of inspection signal. The result obtained many frequency constituents. The defects characterization was still accompanied with the noise at high frequency constituents. Thus, the DWT was used to de-noise them for better inspection results.

**De-noising with DWT**

The DWT was implemented to de-noise the MFL inspection signal by decomposition of the frequency constituents of the signal. The decomposition process was capable to iterate in multi-level of resolution components. Because the low frequency constituent is a very

significant component of the MFL signal, the DWT was used for analyzing. The suitable level of decomposition is based on the nature of the signal, or on a suitable criterion. The LF signal in this paper obtained the high frequency noises, but their amplitude was not very high. Therefore 3 levels of the wavelet decomposition tree are suitable for de-noising the inspection signal. In Figure 12 is shown the 3 levels of wavelet decomposition tree for de-noising the MFL inspection signal.

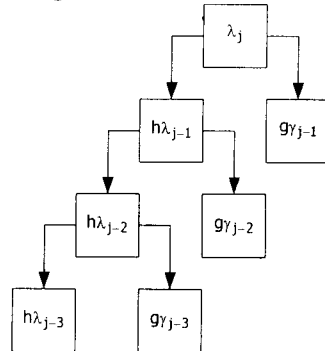


Figure 12 the wavelet decomposition tree

The decomposition analysis in 3 levels has been utilized to de-noise the MFL signal. Whereas the decomposed signal is

$$\lambda_j = \gamma_{j-1} + \gamma_{j-2} + \gamma_{j-3} + \lambda_{j-3} \quad (17)$$

The inspection signal  $\lambda_j$  was decomposed by the high pass filter  $g(k)$  in level  $\gamma_{j-3}$  and the low pass filter  $h(k)$  in level  $\lambda_{j-3}$  too. The de-noising result by DWT has been shown in the decomposition 3 levels of the frequency constituents in Figure 13.

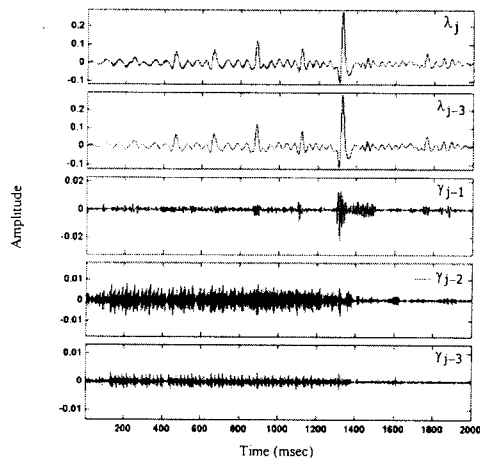


Figure 13 Decomposition of the MFL signal using DWT in level 3

The consequence result of the DWT has demonstrated the 3 levels of decomposed signal. The high frequency of noise constituents was filtered by the high-pass filter  $g(k)$ . It was able to show that the noise in high frequency is caused from the electromagnetic disturbance, analog electronic circuits and electrical signal of the MFL equipment. Output from de-noising is the low pass filtered signal  $\lambda_{j-3}$  in level 3. The 10 defects of the wire rope can be easily analyzed and observed after the inspection signal has been de-noised. The advantage of the DWT is the inspection signal can be iteratively decomposed in many levels. The frequency constituents of the signal can be successively analyzed in every scale in multi resolutions.

The product of the wavelet transform processes has revealed the characterization and de-noising of the wire rope MFL signal by using continuous and discrete wavelet transform. The wire rope defects can be investigated in the different revelation of the inspection signal. In Figure 14 the 3D visualization of the CWT has completely established the time-frequency presentations of the wire rope MFL inspection signal. The good visualization of the 10 defects has been shown in the time and frequency localizations of the inspection signal. Figure 15 has shown the inspection LF signal was de-noised by using DWT. It was decomposed in 3 levels which is good revelation the defects signal of the wire rope.

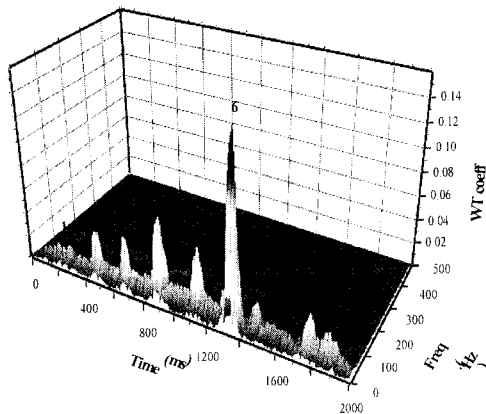


Figure 14 time-frequency presentations of the MFL inspection signal in 3D

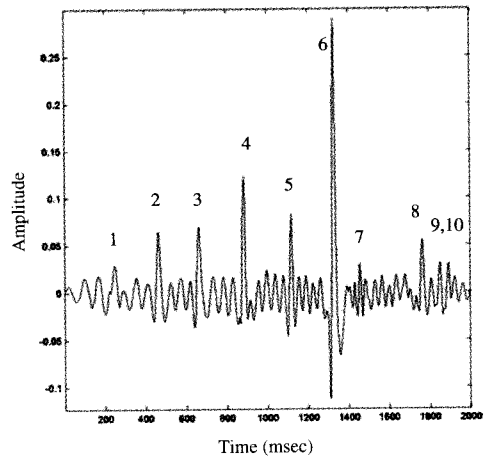


Figure 15 The LF signal was de-noised by DWT

## 6. Conclusions

MFL equipment has been designed and constructed to monitor LF and LMA of wire ropes. Coil censor was studied and selected to detect the flux leakage from defects. The performance of the equipment has been tested and represented by good resolution, repeatability and sensitivity. From the research, the equipment has been able to display the results of LF and LMA signal in an oscilloscope simultaneously.

The LF signal was established to analyze using the wavelet transform. The continuous wavelet transform (CWT) was implemented to characterize the defect signal in the 2D and 3D time-scale presentations. The time and frequency localizations of the defects have been demonstrated in better visualization of the multi resolution. To improve the inspection signal, the high frequency components were necessarily removed from the interested signal. As well, the discrete wavelet transform (DWT) has been used to de-noise the inspection signal. It can be established with decomposition the frequency constituents of the signal. Consequently the defects of the wire rope can be characterized and analyzed for revelation of the wire rope MFL inspection.

## References

- [1] Bethlehem Wire Rope, Bethlehem Mining Product, Williamsport Wirerope Works Inc, 2000
- [2] Weischedel, H.R., The Inspection of Wire Ropes in Service: A Critical Review, Material Evaluation, Vol.43, No.13, pp. 1592-1605, 1985.
- [3] S.D. Singh, and B. Ghara, Steel Wire Rope Condition Monitoring by Non-destructive Investigation, Proceeding of WCNDT Conference, Roma, 2000.
- [4] Moriya, T., Tsukada, K. and Hanasaki, K., A Magnetic Method for Evaluation of Deterioration of Large Diameter Wire Ropes, Proceeding of WCNDT Conference, Roma, 2000.
- [5] Barat, V., Slesarev, D. and Lunin, V., Wavelet Analysis of MFL Signal for Steel Wire Rope Testing, Proceeding of WCNDT Conference, Roma, 2000.
- [6] Lijian, Y., Haiying, F. and Yumei, W., The Application of Wavelet Transform in Magnetic Flux Leakage Test of Pipeline, 10<sup>th</sup> APCNDT, Brisbane, 2001.
- [7] Mukhopadhyay, S. and Srivastava, G.P., Characterisation of Metal Loss Defects from Magnetic Flux Leakage Signals with Discrete Wavelet Transform, NDT&E International, Vol. 33, pp. 57-65, 2000.
- [8] Afzal, M. and Udpa, S., Advance Signal Processing of Magnetic Flux Leakage Data Obtained from Seamless Gas Pipeline, NDT&E International, Vol. 33, pp. 57-65, 2000.
- [9] Jomdecha, C., Prateepasen, A. and Methong, W., Design and Construction of Magnetic-Flux-Leakage Equipment for Detecting Localized Faults of Wire Rope, MSAT 2, MTEC, pp.76-78, 2002.
- [10] Jomdecha, C., Prateepasen, A. and Methong W., Localized Faults of Wire Rope by Magnetic Flux Leakage Inspection, EECON 25, 21-22 November 2002, Prince of Songkla University, Hatyai, Thailand, pp. GN 11-15, 2002.
- [11] Jomdecha, C., Prateepasen, A. and Methong W., Coil Sensors for Wire Rope Inspection using Magnetic Flux Leakage Instrument, ICCAS 2002, 16-19 October 2002, Muju Resort, Jeonbuk, Korea, pp. 1131-1136, 2002.
- [12] EMPA Uberlandstrasse Co., The Presentation Notes of Inspection Stay Cables of RAMA IX Bridge to ETA Staff, 2001.
- [13] Jianxing, C., and Wei, G., The Principle and Application of a New Technique for Detecting Wire Rope Defects, IEEE Conference on Industrial Technology, pp. 445-449, 1996.
- [14] The ASTM E1571-01, Standard Practice for Electromagnetic Examination of Ferromagnetic Steel Wire Rope, ASTM Standard, Vol. 3.03, Section 15, pp. 848-852, 2001.
- [15] Polikar, R., The Wavelet Tutorial: Fundamental Concepts an Overview of The Wavelet Theory, Rowan University, 1994.
- [16] Valen, C., A Really Friendly Guide to Wavelets, Vallen-Systeme GmbH, Germany, 1999.
- [17] Graps, A., An Introduction to Wavelets, IEEE Computational Science and Engineering, 1995.
- [18] Daubechies, I., Ten Lectures on Wavelets, Society for Industrial and Applied Mathematics, Philadelphia, PA, 1992.